Inorg. Chem. **2008**, *47*, 11763−11773

Mononuclear Ruthenium(II) Complexes That Catalyze Water Oxidation

Huan-Wei Tseng,[†] Ruifa Zong,[†] James T. Muckerman,[‡] and Randolph Thummel*[,†]

Department of Chemistry, University of Houston, 136 Fleming Building, Houston, Texas 77204-5003, and Chemistry Department, Brookhaven National Laboratory, Upton, New York 11973-5000

Received August 5, 2008

Two series of mononuclear ruthenium(II) complexes involving polypyridine-type ligands have been prepared, and their ability to act as catalysts for water oxidation has been examined. One series is of the type $[Ru(tpy)(NN)Cl](PF_6)$ (tpy = 2,2′; 6,2″-terpyridine), where NN is one of 12 different bidentate ligands, and the other series includes various combinations of 4-picoline, 2,2′-bipyridine (bpy), and tpy as well as the tetradentate 2,9-dipyrid-2′-yl-1,10-phenanthroline (dpp). The electronic absorption and redox data for these compounds have been measured and reported. The long-wavelength metal-to-ligand charge-transfer absorption and the first oxidation and reduction potentials are found to be consistent with the structure of the complex. Of the 23 complexes, 14 catalyze water oxidation and all of these contain a tpy or dpp. Kinetic measurements indicate a first-order reaction and together with a catalyst recovery experiment argue against the involvement of RuO_2. A tentative mechanism is proposed that involves a seven-coordinate Ru^{VI}═O species that is attacked by water to form the critical O−O bond. Density functional theory calculations, which support the proposed mechanism, are performed.

Introduction

The efficient production of nonfossil-based, environmentally friendly fuels is one the biggest challenges ever faced by modern science.[1] A wide variety of approaches are under study, and many of these approaches use sunlight as the source of energy needed to produce the fuel. In effect, such a process might drastically shorten the time scale involved in the natural process by which fossil fuels are derived through photosynthesis.[2] A very attractive fuel is hydrogen because it embodies high energy content and combusts to form water as the only byproduct. The source of most of the hydrogen produced today is low-molecular-weight hydrocarbons. What is desired is to replace this source with the much more abundant, and virtually free, water. In order to decompose water to provide hydrogen in a catalytic manner, we must also make oxygen, and it is the loss of four electrons in the oxidation step (eq 1) that presents the most serious challenge to catalytic water decomposition.

$$2OH^- - 4e^- \rightarrow O_2 + 2H^+ \quad (1)$$

Metal complexes having a variety of available redox states present attractive possibilities as potential water oxidation catalysts. Polypyridine complexes of ruthenium(II) and other transition metals have been extensively studied in this regard.[3] One of the first examples of a ruthenium-based catalyst capable of water oxidation was the so-called "blue dimer" prepared by Meyer and co-workers in the early 1980s.[4] This species was characterized as *cis*,*cis*-$[(bpy)_2(H_2O)Ru^{III}ORu^{III}(OH_2)(bpy)_2]^{4+}$ (bpy = 2,2′-bipyridine), having the identical halves of the complex linked by an oxo bridge. The water molecules were situated cis to one another such that it was attractive to suggest that dioxygen might be evolved from an oxygen atom associated with each of the two metals. A strong sacrificial oxidant [cerium(IV)] is required to activate the catalyst, and under these conditions,

* To whom correspondence should be addressed. E-mail: thummel@uh.edu.
† University of Houston.
‡ Brookhaven National Laboratory.

(1) Directing Matter and Energy: Five Challenges for Science and the Imagination. Report from the Basic Energy Sciences Advisory Committee, Sept 20, 2007.
(2) Office of Science, Department of Energy. Report of the Basic Energy Sciences Workshop on Solar Energy Utilization, Apr 18−21, 2005.
(3) (a) Alstrum-Acevedo, J. H.; Brennaman, M. K.; Meyer, T. J. *Inorg. Chem.* **2005**, *44*, 6802–6827. (b) Yagi, M.; Kaneko, M. *Chem. Rev.* **2001**, *101*, 21–35. (c) Rüttinger, W.; Dismukes, G. C. *Chem. Rev.* **1997**, *97*, 1–24. (d) Che, C.-M.; Ho, C.; Lau, T.-C. *J. Chem. Soc., Dalton Trans.* **1991**, 1901–1907.

10.1021/ic8014817 CCC: $40.75
Published on Web 11/12/2008

turnover numbers (TNs) were low.[5] An elegant attempt was made to stabilize the complex by using two bipyridines linked at the 4 position with a polymethylene bridge.[6] It was expected that if the oxo bridge broke during the water oxidation process, the remaining bridge between the bpy moieties would entropically favor re-formation of the critical oxo linkage. No remarkable improvement in the activity was observed for this linked catalyst.

In 2004, Llobet and co-workers reported a new water oxidation catalyst in which two Ru(tpy) centers (tpy = 2,2′;6,2″-terpyridine) were bridged by a bis-bidentate dipyridylpyrazole.[7] The metals were situated close enough to accommodate an acetate linker between them. It was postulated that in the presence of cerium(IV) this acetate was replaced by two water molecules, which eventually gave rise to dioxygen and protons released to solution. Again, however, the TNs were modest.

A more active dinuclear ruthenium water oxidation catalyst was reported in 2001 by Tanaka and co-workers.[8] This system used a 1,8-anthracenyl linker to situate two tpy's face-to-face. The remaining coordination sites were occupied by a hydroxide and a disubstituted derivative of *o*-benzoquinone. Electrochemical activation of the catalyst resulted in a TN of 33 500 after 40 h of operation, and the mechanism of this process recently has been studied.[9] Earlier this year, two groups independently reported a completely inorganic tetranuclear ruthenium cluster active in water oxidation with a turnover efficiency measured at 18−500.[10,11] In 2005, we reported a series of chloro-bridged diruthenium complexes (**1a**−**c**) in which the two metal centers are held in close proximity by a bis-tridentate ligand.[12] It was remarkable that the seven components of this complex self-assembled to form a single discrete species in yields approximating 50%. Upon exposure to aqueous cerium(IV) at pH 1, this complex catalyzed the copious evolution of oxygen with TNs in the range of 112−538.[13] In a structure−activity study aimed at optimizing the performance, we varied both the axial and equatorial ligands, examining 14 different complexes.[14] The maximum TN was 689 for the 4-methoxypyridine analogue of **1**, while two systems with *N*-methylimidazole as the axial ligand were completely inactive.

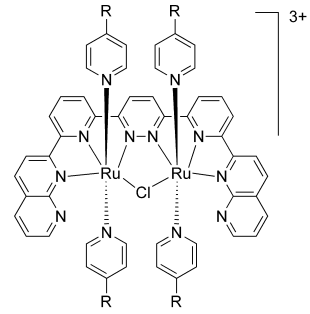

1a R = CH_3 (TN = 538)
b R = CF_3 (TN = 116)
c R = NMe_2 (TN = 112)

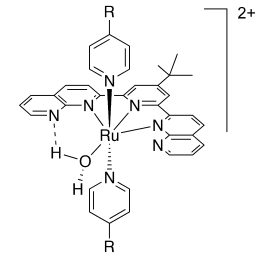

2a R = CH_3 (TN = 260)
b R = CF_3 (TN = 35)
c R = NMe_2 (TN = 20)

From our own work and that of others, we initially presumed that two proximal ruthenium centers were critical for oxygen generation. To test this theory, we examined the series of mononuclear complexes **2**, which closely resembled half of the dinuclear catalyst **1**. Surprisingly, these mononuclear complexes showed good catalytic activity with TNs in the range of 20−260.[12,13] For both **1** and **2**, the substituent effects are consistent with the 4-picoline (pic)-substituted systems **1a** and **2a** being the most active. Under the low-pH conditions for oxygen generation, the dimethylamino substituent of **1c** and **2c** is likely protonated and thus behaves similarly to the electron-withdrawing trifluoromethyl group.

We reasoned that the structurally more simple mononuclear catalyst might be a better starting point in our attempts to understand and optimize these water oxidation catalysts; thus, we undertook a careful study of several series of mononuclear systems, and this paper will report the results of that study.

Systems To Be Studied

In this study, we examine 20 mononuclear ruthenium(II) complexes. Some of these complexes (**3**−**10**) are derivatives of $[Ru(bpy)(tpy)Cl]^+$, where the nature of the bidentate ligand has been varied to include five different 4,4′-disubstituted bpy's (**3a**−**e**), several benzo-annelated derivatives of bpy (**4**−**7**), two diaza analogues of bpy (**8** and **9**), and a pyrido-fused bpy (**10**) (Scheme 1). The second group of complexes are coordinatively saturated with pyridine-type ligands in which both the number and the denticity of the ligands are varied to include 1−3 bpy's, 1 or 2 tpy's, and 1−4 pic's, as well as the tetradentate 2,9-dipyrid-2′-yl-1,10-phenanthroline (dpp; Scheme 2).[15]

(4) (a) Gersten, S. W.; Samuels, G. J.; Meyer, T. J. *J. Am. Chem. Soc.* **1982**, *104*, 4029–4030. (b) Gilbert, J. A.; Eggleston, D. S.; Murphy, W. R.; Geselowitz, D. A.; Gersten, S. W.; Hodgson, D. J.; Meyer, T. J. *J. Am. Chem. Soc.* **1985**, *107*, 3855–3864. (c) Raven, S. J.; Meyer, T. J. *Inorg. Chem.* **1988**, *27*, 4478–4483. (d) Geselowitz, D.; Meyer, T. J. *Inorg. Chem.* **1990**, *29*, 3894–3896. (e) Chronister, C. W.; Binstead, R. A.; Ni, J.; Meyer, T. J. *Inorg. Chem.* **1997**, *36*, 3814–3815. (f) Lebeau, E. L.; Adeyemi, S. A.; Meyer, T. J. *Inorg. Chem.* **1998**, *37*, 6476–6484. (g) Binstead, R. A.; Chronister, C. W.; Ni, J.; Hartshorn, C. M.; Meyer, T. J. *J. Am. Chem. Soc.* **2000**, *122*, 8464–8473. (h) Yang, X.; Baik, M.-H. *J. Am. Chem. Soc.* **2004**, *126*, 13222–13223. (i) Lei, Y.; Hurst, J. K. *Inorg. Chim. Acta* **1994**, *226*, 179–185. (j) Yamada, H.; Siems, W. F.; Koike, T.; Hurst, J. K. *J. Am. Chem. Soc.* **2004**, *126*, 9786–9795.
(5) Collin, J. P.; Sauvage, J. P. *Inorg. Chem.* **1986**, *25*, 135–141.
(6) Petach, H. H.; Elliott, C. M. *J. Electrochem. Soc.* **1992**, *139*, 2217–2221.
(7) Sens, C.; Romero, I.; Rodriguez, M.; Llobet, A.; Parella, T.; Benet-Buchholz, J. *J. Am. Chem. Soc.* **2004**, *126*, 7798–7799.
(8) (a) Wada, T.; Tsuge, K.; Tanaka, K. *Inorg. Chem.* **2001**, *40*, 329–337. (b) Wada, T.; Tsuge, K.; Tanaka, K. *Angew. Chem., Int. Ed.* **2000**, *39*, 1479–1482.
(9) Muckerman, J. T.; Polyansky, D.; Wada, T.; Tanaka, K.; Fujita, E. *Inorg. Chem.* **2008**, *47*, 1787–1802.
(10) (a) Geletii, Y. V.; Botar, B.; Kögerler, P.; Hillesheim, D. A.; Musaev, D. G.; Hill, C. L. *Angew. Chem., Int. Ed.* **2008**, *47*, 3896–3899. (b) Sartorel, A.; Carraro, M.; Scorrano, G.; De Zorzi, R.; Geremia, S.; McDaniel, N. D.; Bernhard, S.; Bonchio, M. *J. Am. Chem. Soc.* **2008**, *130*, 5006–5007.
(11) Süss-Fink, G. *Angew. Chem., Int. Ed.* **2008**, *47*, 5888–5890.
(12) Zong, R.; Thummel, R. P. *J. Am. Chem. Soc.* **2005**, *127*, 12802–12803.
(13) These numbers are lower than some of those reported previously (ref 12) because of modification in the method of oxygen measurement (ref 14).
(14) Deng, Z.; Tseng, H.-W.; Zong, R.; Wang, D.; Thummel, R. *Inorg. Chem.* **2008**, *47*, 1835–1848.

Scheme 1

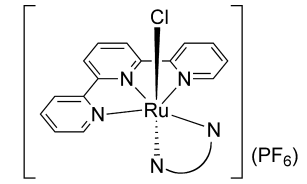

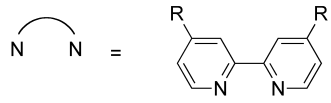

3a R = H

3b R = Me

3c R = OMe

3d R = NO_2

3e R = COOEt

4

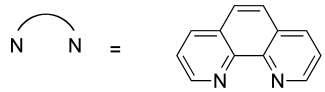

5

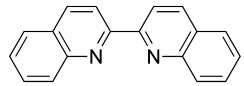

6

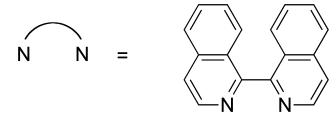

7

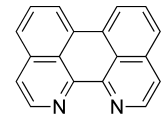

8

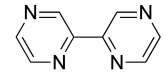

9

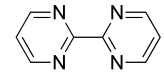

10

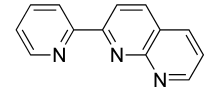

Scheme 2

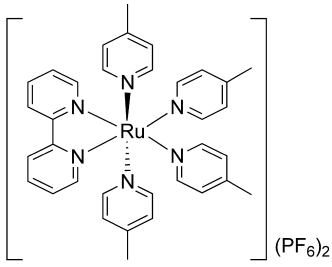

11

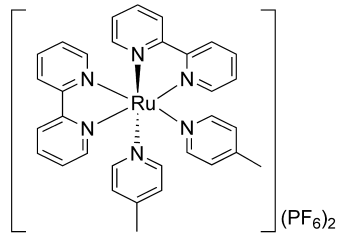

12

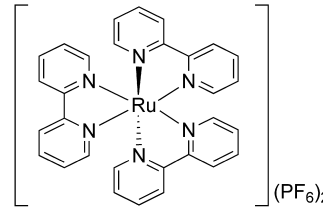

13

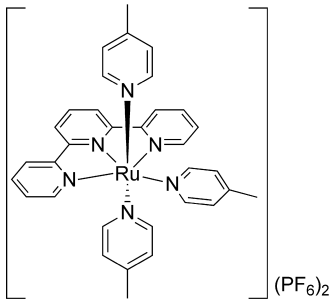

14

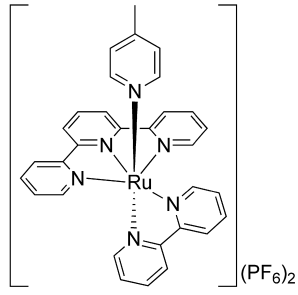

15

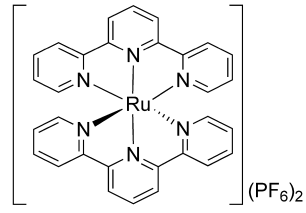

16

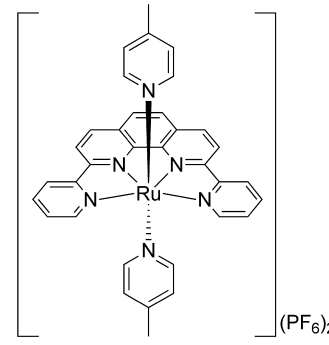

17

Many of these complexes have been reported previously, and they were prepared according to literature methods. The complexes **3d**, **3e**, **7**, **10**, **11**, **14**, and **15** were unknown, and they were synthesized in a manner analogous to that reported for other similar members of the same series. Because of higher symmetry and the existence of discrete 2 and 3 spin ^{1}H NMR patterns, all of the complexes could be identified unambiguously by ^{1}H NMR. To further characterize these systems, we measured their electronic absorption spectra and their redox potentials and these data are collected in Table 1.

Table 1. Electronic Absorption[a] and CV[b] Data for Complexes **3**−**17**

complex	λ_{max}, nm (ϵ, M^{-1} cm^{-1})	$E_{1/2}^{ox}$ (ΔE)	$E_{1/2}^{red}$ (ΔE)
3a	363 (7420), sh, 508 (10 742)	0.80 (74)	−1.44 (99), −1.59 (103)
3b	365 (6604), sh, 511 (9006)	0.76 (79)	−1.47 (102), −1.65 (93)
3c	368 (7828), 518 (9670)	0.70 (76)	−1.49 (108), −1.66 (80)
3d	467 (12 332), sh, 549 (16 834)	1.03 (74)	−0.57 (75), −0.70 (73)
3e	394 (9916), 528 (16 618)	0.92 (89)	−1.15 (81), −1.47 (189), −1.79[ir]
4	439 (7376), sh, 506 (11 014)	0.81 (101)	−1.38 (227), −1.59 (91)
5	586 (11 912)	0.90 (87)	−1.06 (79), −1.38 (73), −1.59 (98)
6	359 (18 010), 569 (15 468)	0.81 (73)	−1.09 (83), −1.47 (102), −1.73[ir]
7	412 (8846), 446 (13 924), 472 (17 002), 600 (19 944)	0.83 (83)	−0.86 (83), −1.44 (52), −1.80[ir]
8	370 (7106), 517 (13 188)	1.03 (71)	−1.06 (76), −1.55[ir]
9	371 (8190), 520 (8572)	0.91 (75)	−1.16 (81), −1.59[ir]
10	368 (6156), sh, 568 (10 978)	0.76 (86)	−1.13 (76), −1.49[ir], −1.74[ir]
11	475 (4222)	1.18 (83)	−1.39 (75)
12	471 (8468)	1.24 (80)	−1.37 (85), −1.59 (99)
13	393 (5974), sh, 422 (12 162), sh, 452 (15 272)	1.28 (83)	−1.35 (73), −1.54 (84), −1.78 (86)
14	453 (4444), sh, 503 (6044), 558 (2424), sh, 619 (888), sh	1.22 (86)	−1.27 (83), −1.81[ir]
15	416 (4666), sh, 470 (7096), 542 (1384), sh, 592 (628), sh	1.22 (74)	−1.26 (87), −1.60 (85)
16	476 (14 582)	1.28 (76)	−1.27 (73), −1.52 (76)
17	406 (3842), 450 (2766), sh, 485 (4208), sh, 543 (6032)	1.25 (76)	−1.06 (76), −1.64[ir]

[a] Measured in acetone (5.0×10^{-5} M). [b] Measured with a glassy carbon electrode at 100 mV s^{-1} in CH_3CN containing 0.1 M NBu_4PF_6 and reported in volts related to SCE; $E_{1/2} = (E_{pa} + E_{pc})/2$ in volts, and $\Delta E = (E_{pa} - E_{pc})$ in millivolts; ir = irreversible.

In the series of closely related disubstituted derivatives of $[Ru(tpy)(bpy)Cl]^+$ (**3a**−**e**), the characteristic long-wavelength absorption is attributed to a metal-to-ligand charge transfer (MLCT). When the 4,4′ substituents are electron-withdrawing as in **3d** and **3e**, this band is shifted to longer wavelength. At the same time, the ligand-centered first reduction becomes more positive, which is also consistent with a lowering of the energy of the π^* orbital. This electronegativity would similarly destabilize the ruthenium(III) state and thus leads to an increase in the oxidation potential for **3d** and **3e**.

For the series of complexes **4**−**7**, the properties of the phenanthroline derivative **4** are quite similar to those of the parent bpy system. The biquinoline and biisoquinoline derivatives **5** and **6** show a red shift of the MLCT band as well as an increase in the first reduction potential. For the even more delocalized diazaperylene system **7**, the MLCT has moved to 600 nm and the reduction potential has increased to −0.86 V. Interestingly, the oxidation potentials for this series do not appear to be as sensitive to the changes in the ligand π system. The two systems **8** and **9**, where 2,2′-bipyrazine and 2,2′-bipyrimidine have been substituted for bpy, show behavior that is similar to the electronegative bpy systems **3d** and **3e**.

The series of complexes **11**−**17** all have six pyridine-type rings coordinated to the metal center, but the denticity of the ligands is varied. With the exception of the somewhat higher reduction potential for **17**, the other complexes show first reduction and oxidation properties that fall within a 120 mV range of one another. The absorption spectra show components for MLCT to 4-picoline at higher energy and bpy or tpy at lower energy. The series **11**−**13** is especially well behaved, with the high-energy component decreasing with fewer picolines and the low-energy bpy component becoming more intense as the number of bpy's is increased from one to three (Figure 1).

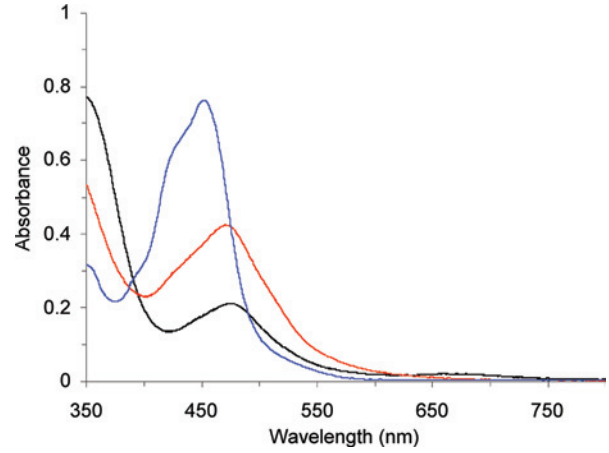

Figure 1. Electronic absorption spectra recorded in acetone (5×10^{-5} M): **11** (black), **12** (red), and **13** (blue).

Water Oxidation

In our initial report on ruthenium-catalyzed water oxidation, we cited TNs for **2a**−**c** that were measured with a YSI electrochemical oxygen probe. In a subsequent paper, we pointed out some shortcomings of this method, and we have now replaced the YSI electrode with a more sturdy and reliable optical probe whose response is based on oxygen quenching of a ruthenium complex at the probe tip. Kinetic measurements taken with this probe are verified by end-point readings measured by gas chromatography (GC). Thus, the first three entries in Table 2 are corrected somewhat downward from our earlier reported values for **2a**−**c**. Nevertheless, the system **2a** having two axial 4-picoline ligands is considerably more active than the analogues where the axial pyridines bear a 4 substituent that is electronegative. At pH 1, the dimethylamino group would be protonated and thus electron-withdrawing. On the basis of this observation, in subsequent studies we have used picoline exclusively as the monosubstituted ligand.

To draw better conclusions from the data in Table 2, we considered the catalysts in several structurally related groups. We looked first at the group **3a**−**e** in which the 4,4′

(15) Zhang, G.; Zong, R.; Tseng, H.-W.; Thummel, R. P. *Inorg. Chem.* **2008**, *47*, 990–998.

Table 2. TN and Rate Data for Complexes **2**−**17** and **24**

complex	TN	rate (μmol min^{-1})
2a	260	0.169[a]
2b	35	0.039[a]
2c	20	0.018[a]
3a	390	0.356[a]; 0.334[b]
3b	190	0.474[b]
3c	110	0.383[b]
3d	260	0.044[b]
3e	570	0.102[b]
4	400	0.318[a]
5	0[c]	
6	0[c]	
7	0[c]	
8	0[c]	
9	0[c]	
10	1170	0.403[a]
11	0[c]	
12	0[c]	
13	0[c]	
14	95	0.021[a]
15	135	0.042[a]
16	0[c]	
17	416	0.330[a]
24	260	0.138[a]

[a] A second-order polynomial was used to fit the generated oxygen vs time curves (Figures 2 and 4) in the period of 0−60 min; rate = slope of the curve at 30 min. [b] A second-order polynomial was used to fit the generated oxygen vs time curves (Figures 2 and 4) in the period of 0−30 min; rate = slope of the curve at 15 min. [c] Too low to measure under the general reaction conditions.

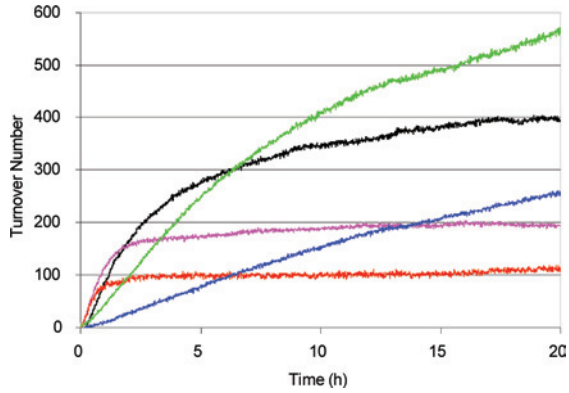

Figure 2. Kinetic plots of oxygen evolution vs time for **3a** (black), **3b** (lavender), **3c** (red), **3d** (blue), and **3e** (green).

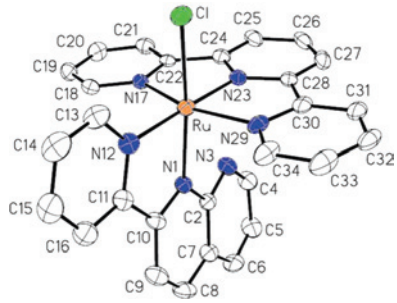

Figure 3. ORTEP drawing of the cation of **10**, showing the atom numbering scheme. Hydrogen atoms are omitted for clarity.

substituent is varied on the bpy ligand of the parent complex $[Ru(tpy)(bpy)Cl]^+$ (**3a**). All five of these catalysts show good activity with TNs in the range of 110−570. The kinetic curves for 20 h runs are plotted in Figure 2. Interestingly, unlike what we observed for the dinuclear ruthenium catalysts, there appears to be almost a reverse relationship between the rate and TN. The fastest systems, **3b** and **3c**, have the lowest TNs, while **3e**, which proceeds at a modest rate, gives the highest TN.

The second group of potential catalysts (**4**−**9**) again are analogues of $[Ru(tpy)(bpy)Cl]^+$ but where the bpy has now been substituted with a more delocalized, benzo-substituted derivative or a diaza analogue of bpy (bipyrazine or bipyrimidine). The system $[Ru(tpy)(phen)Cl]^+$ (**4**) behaves almost the same as the parent bpy system, and this is not too surprising because the photo- and electrochemical properties of Ru(bpy) and Ru(phen) complexes are quite similar.[16] The other five complexes are unreactive within the sensitivity of our method, which could easily detect a TN ≥ 10. System **10** is an anomaly. The 2-(pyrid-2′-yl)-1,8-naphthyridine (pynap) ligand differs from all of the other bidentates in that it is unsymmetrical. It would seemingly combine the delocalization and electronegativity properties of the bidentates in complexes **4**−**9**, yet it is far more reactive and shows the highest TN for any system, mono- or dinuclear, that we have measured to date.

For complex **10**, there is a stereochemistry question with regard to binding of the pynap ligand.[17] In an earlier study, we determined that $[Ru(tpy)Cl_3]$ reacts with other polypyridine ligands such that the initial attack is preferred in the equatorial plane occupied by the tpy.[18] The pynap ligand would therefore attack first with its more basic pyridine ring in this plane, situating the naphthyridine ring and chloride trans to one another. This stereochemistry is verified by ^{1}H NMR, which indicated H6 on the pyridine of pynap far downfield at 10.61 ppm due to deshielding by the proximal chlorine. We verified this situation with an X-ray structure analysis of **10**. Figure 3 shows an ORTEP drawing of the cation of this complex, and Table 3 summarizes some of the pertinent geometric features.

The Ru−N distances all fall in the range of 2.065−2.075 Å with the exception of the central Ru bond to tpy, which is shorter (1.961 Å), as expected. The bite angle to pynap (78.09°) is slightly less than the bite angles to tpy, which average 79.62°. The bound ligands are close to planar. The dihedral angle is estimated by the average of the two torsion angles about the inter-ring bond. For pynap, this angle is about 3.5°, and for tpy, the two dihedral angles average about 1.9°. Interaction between the naphthyridine and tpy rings causes some distortion of the octahedral geometry such that the N1−Ru−N23 angle opens up to 101.53° and the N1−Ru−Cl bonds are nonlinear at 171.22°.

The final group of complexes to be examined for catalytic activity were **11**−**17**, in which the number of pyridines, bpy's, and tpy's are varied in a regular fashion. System **17** includes a tetradentate dipyridyl phen whose catalysis of water oxidation we have reported previously.[15] Systems **11**−**13**, which contain one, two, or three bpy's and a complementary number of pic's, are all inactive. However,

(16) Juris, A.; Balzani, V.; Barigelletti, F.; Campagna, S.; Belser, P.; von Zelewsky, A. *Coord. Chem. Rev.* **1988**, *84*, 85.
(17) Hartshorn, C. M.; Maxwell, K. A.; White, P. S.; DeSimone, J. M.; Meyer, T. J. *Inorg. Chem.* **2001**, *40*, 601–606.
(18) Jahng, Y.; Thummel, R. P.; Bott, S. G. *Inorg. Chem.* **1997**, *36*, 3133–3138.

Table 3. Selected Geometric Data for Complex **10**

		Bond Lengths (Å)			
Ru−N1	2.070(3)	Ru−N12	2.075(3)	Ru−N17	2.065(2)
Ru−N23	1.961(3)	Ru−N29	2.071(3)	Ru−Cl	2.4179(10)
		Bond Angles (deg)			
N1−Ru−N12	78.09(11)	N1−Ru−N17	92.87(10)		
N23−Ru−N29	79.70(11)	N1−Ru−N29	90.50(10)		
N23−Ru−N17	79.54(10)	N1−Ru−N23	101.53(11)		
N23−Ru−Cl	87.06(8)	N1−Ru−Cl	171.22(8)		
		Torsion Angles (deg)			
N1−C10−C11−N12	−3.1(4)	C9−C10−C11−C16	−4.0(5)		
N17−C22−C24−N23	2.9(4)	C21−C22−C24−C25	0.8(6)		
N23−C28−C30−N29	1.3(4)	C27−C28−C30−C31	2.7(6)		

14 and **15**, which each contain a single tpy, are both moderately active, while **17** shows good activity (TN = 416; Figure 4).

Mechanism

Before one can seriously consider possible mechanisms whereby these catalysts function to decompose water, the possible involvement of ruthenium dioxide must be addressed. Under strongly oxidizing conditions, it is possible that the ligands that surround ruthenium could be oxidized, destroying the complex and affording ruthenium dioxide, which could then function as a heterogeneous water oxidation catalyst. Previous workers have commented on this possibility[5,19] and in several instances have noticed the formation of a black insoluble material, which they tentatively assign as RuO_2. Because of its poor solubility and rather lackluster physical properties, RuO_2 is not an easy species to identify. We have carried out several experiments to help investigate this question.

We have substituted $RuCl_3$ and $Ru(DMSO)_4Cl_2$ as the catalyst under our typical reaction conditions and have not observed the generation of any oxygen. If we use a commercial sample RuO_2, we do see oxygen evolution, but both the rate and TN are low. Figure 4 shows a comparison of the kinetic runs for four catalysts including RuO_2. The complexes **14** and **15** show oxygen evolution curves that are very similar to the one obtained for RuO_2, making them somewhat suspect in this regard. The catalyst **17**, on the other hand, shows a much faster rate and a higher TN, not at all resembling RuO_2. Alternatively, one could argue that catalyst decomposition could afford a more reactive form of RuO_2, which might show better reactivity.

To determine that the catalyst was not being consumed in the reaction, we attempted to recover it after several turnovers. The catalyst [Ru(tpy)(bpy)Cl]Cl (20 mg) was added to 40 equiv (sufficient for 10 turnovers) of ceric ammonium nitrate, and the catalyst color turned immediately from red to green. Oxygen evolution was detected by GC, and after 3 h, excess aqueous NH_4PF_6 was added to precipitate 28 mg of a green solid. A ^1H NMR of the green solid in CD_3CN is shown in Figure 5 (top). The downfield aromatic peaks are broad and poorly resolved, as one might expect for a paramagnetic ruthenium species. When ascorbic acid, a reducing agent, is added to the NMR sample, the solution turns from green to red and the NMR spectrum appears as shown in Figure 5 (bottom). The peak at 10.19 ppm is H6 on the bpy ligand, which is strongly deshielded by the proximal chlorine. The spectrum closely resembles the starting catalyst (Figure S1 in the Supporting Information). The mass spectrum of the green solid was consistent with $[Ru(tpy)(bpy)Cl]^{2+}$ as the major species, and the electronic absorption spectrum closely resembled the species reversibly generated from electrochemical oxidation of $[Ru(tpy)(bpy)Cl]^{+}$ (Figure S2 in the Supporting Information).

Given the presumed cooperativity of two metal centers in the previously examined dinuclear ruthenium water oxidation

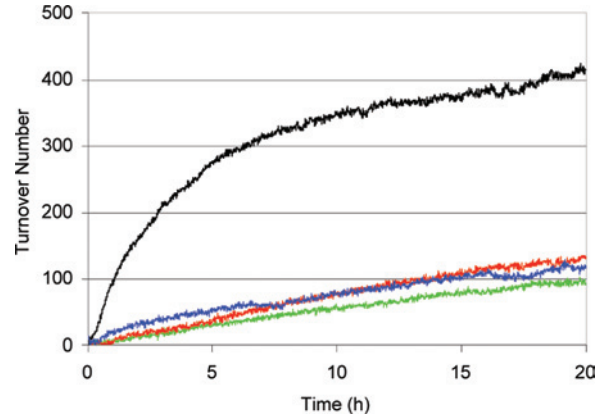

Figure 4. Kinetic plots of oxygen evolution vs time for complexes **14** (green), **15** (red), **17** (black), and RuO_2 (blue).

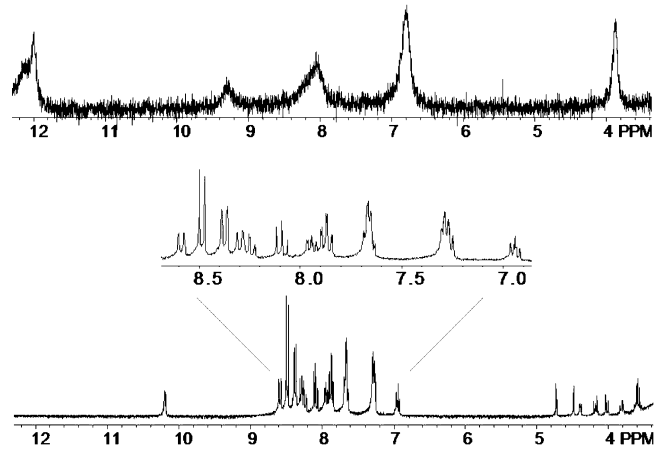

Figure 5. Top: Downfield region of the ^1H NMR spectrum in CD_3CN of the green material precipitated as a PF_6 salt from the water oxidation reaction catalyzed by [Ru(tpy)(bpy)Cl]Cl. Bottom: Same NMR spectrum after the addition of ascorbic acid (ascorbic acid peaks at 3.5−4.8 ppm).

(19) Nagoshi, K.; Yamashita, S.; Yagi, M.; Kaneko, M. *J. Mol. Catal. A: Chem.* **1999**, *144*, 71–76.

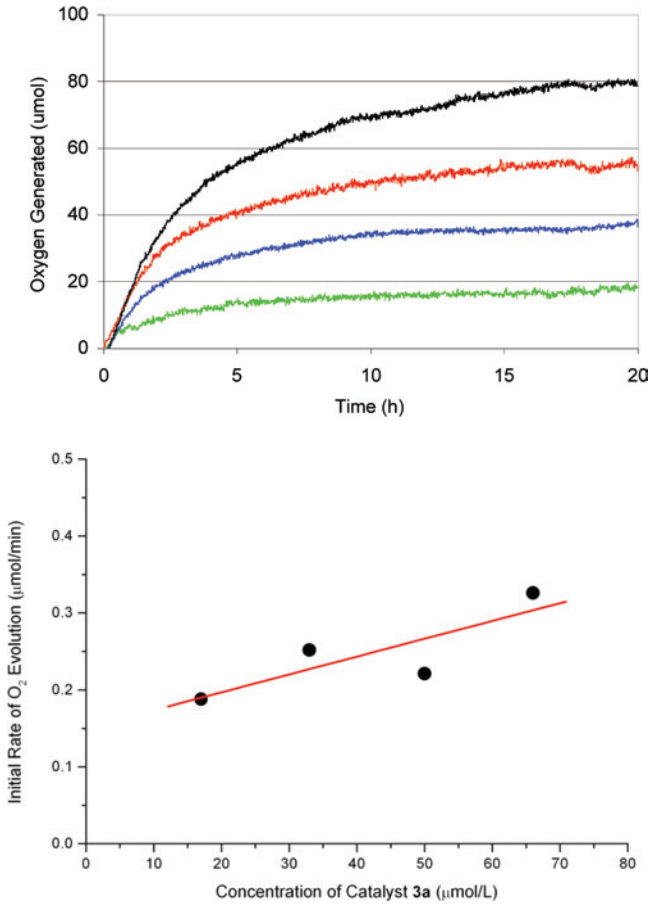

Figure 6. Top: Oxygen evolution vs time at various concentrations of catalyst **3a**: 17 μM (green), 33 μM (blue), 50 μM (red), and 66 μM (black). Bottom: Rate of oxygen evolution ($t = 0$) at various concentratons of **3a**.

catalysts, we were surprised by the high reactivity of some of the mononuclear systems. One possible explanation might involve dimerization of the catalyst perhaps through the formation of a μ-oxo-bridged species. To determine the molecularity of the reaction, we looked at the rates of oxygen evolution catalyzed by **3a** as a function of the catalyst concentration (Figure 6). It is readily apparent that there is a linear dependence of the rate upon the concentration of the catalyst, indicating that the reaction is first order in catalyst so that dimerization is most likely not involved.

As further proof, we prepared a catalyst that would be sterically hindered with regard to possible dimerization. The catalyst was an analogue of **2a**, having two *tert*-butyl groups at the 7′ positions on the 1,8-naphthyridine rings of the equatorial ligand (**23**). The Friedländer condensation of 4-aminopyrimidine-5-carbaldehyde (**18**) with pinacolone provided **20**, which could be hydrolyzed in aqueous HCl to afford 6-*tert*-butyl-2-aminonicotinaldehyde (**21**). A second Friedländer condensation of this material with 4-*tert*-butyl-2,6-diacetylpyridine (**22**) gave the equatorial ligand **23**. A combination of this ligand with $[Ru(DMSO)_4Cl_2]$ followed by 4-picoline and precipitation of the complex with ammonium hexafluorophosphate gave **24**. When this complex is used as a water oxidation catalyst, the results are identical with those obtained with the unsubstituted parent complex **2a**, affording a TN of 260. This result further corroborates the unimolecular nature of the catalytic process.

Although the catalyst appears to survive the oxidation process with all of its original ligands intact, it is difficult to imagine a mechanism whereby water does not at some point coordinate with the metal. To that end, we tentatively propose that if the catalyst loses two electrons upon being oxidized by Ce^{IV} to the Ru^{IV} state, then the metal is surrounded by only 16 electrons and is thus electrophilic and susceptible to attack by water (Scheme 4). Such an attack would afford a high-energy seven-coordinate ruthenium(IV) species. In this intermediate, the L−M−L bite angle should decrease from the 90° optimum of a six-coordinate octahedral ruthenium(II) species. Such a transition would lead to some strain relief for Ru(tpy) and Ru(dpp) complexes and may help to explain the reactivity of this type of complex. There is structural precedence for the formation of a seven-coordinate ruthenium(IV) species, also involving a Ru−Cl bond.[20] The presence of a chloride ligand in some of the active catalysts might also help to increase the electrophilicity of the metal. It is also possible that a single pyridine from a polypyridine ligand could dissociate from the metal without leaving the coordination sphere and then recoordinate to reform the original catalyst. Subsequent loss of two protons and two electrons from the $Ru^{IV}(OH_2)$ species would provide a resonance-stabilized Ru^{VI}═O. Attack of water could then occur at the oxygen of the electrophilic Ru^{VI}═O with the loss of a proton to provide a $Ru^{VI}OOH$ species. Loss of another proton and evolution of dioxygen would regenerate the starting catalyst.

Density Functional Theory (DFT) Calculations

Electronic structure calculations in the gas phase were carried out to optimize the geometry of the catalyst $[Ru^{II}(dpp)(pic)_2]^{2+}$ complex and several of the proposed intermediates derived from it in a catalytic water oxidation cycle. This complex has a six-coordinate, 18-electron metal center, so the first question addressed by the calculations was whether its two-electron-oxidized, 16-electron form could accommodate a water molecule in a seventh-coordination position. The complex was found to do so, and the structure of the resulting seven-coordinate aquo species is shown in Figure S3 in the Supporting Information. The resulting d^4 $Ru^{IV}(OH_2)$ species has the possibility of being either a low-spin singlet or an intermediate-spin triplet, and the calculations indicate that the triplet species is more stable by ca. 10 kcal mol^{-1}. The binding energies, relative to H_2O and singlet and triplet $[Ru^{IV}(dpp)(pic)_2]^{4+}$ for which the triplet is more stable by 6 kcal mol^{-1}, of the H_2O ligand to the singlet and triplet complexes were calculated to be 19 and 23 kcal mol^{-1}, respectively. A related question is whether it is necessary to oxidize the starting ruthenium(II) species in order to coordinate water in a seven-coordinate complex. We therefore

(20) (a) Given, K. W.; Mattson, B. M.; Pignolet, L. H. *Inorg. Chem.* **1976**, *15*, 3152–3156. (b) Given, K. W.; Mattson, B. M.; McGuiggan, M. F.; Miessler, G. L.; Pignolet, L. H. *J. Am. Chem. Soc.* **1977**, *99*, 4855–4857. (c) Wheeler, S. H.; Mattson, B. M.; Miessler, G. L.; Pignolet, L. H. *Inorg. Chem.* **1978**, *17*, 340–350.

Scheme 3

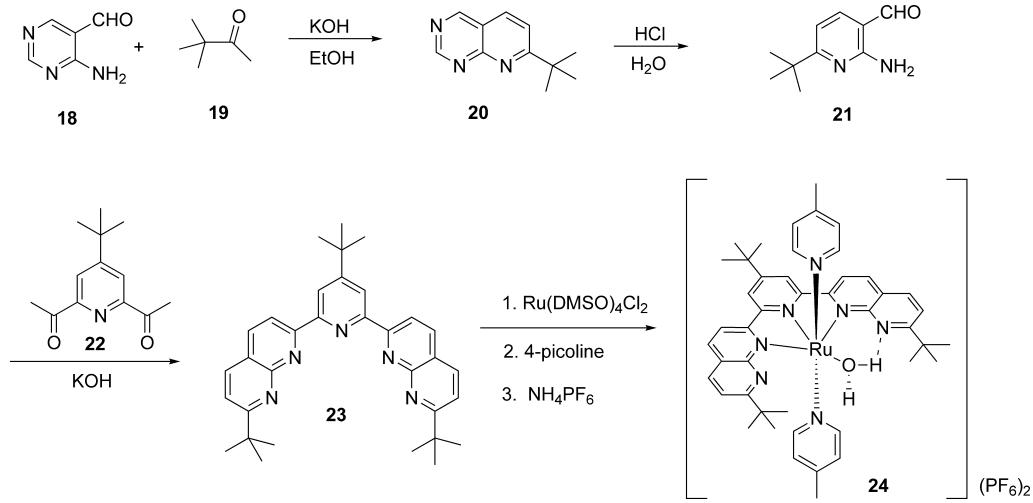

Scheme 4

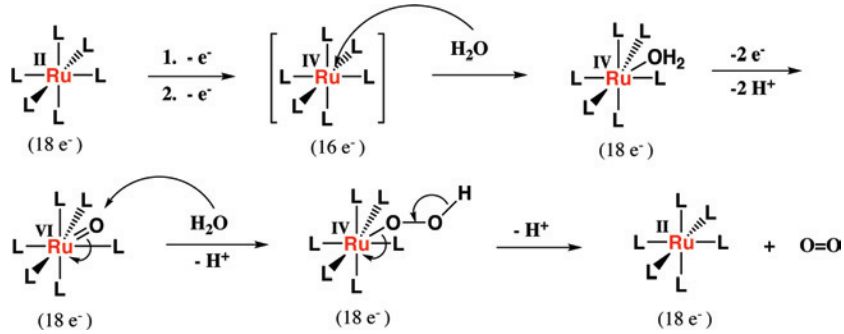

carried out geometry optimization calculations of the $Ru^{II}(OH_2)$ complex starting at the $Ru^{IV}(OH_2)$-optimized geometry. The water molecule was observed to dissociate from the complex during the geometry optimization rather than retaining a 20-electron metal center. A similar calculation on a singly oxidized $Ru^{III}(OH_2)$ complex also led to the dissociation of water.

We then explored the geometry of the $[Ru^{VI}{=}O(dpp)(pic)_2]^{4+}$ species resulting from the removal of the two water protons coupled with two-electron oxidation. Figure S4 in the Supporting Information shows that the calculated structure is essentially a pentagonal bipyrimid, with the oxo ligand in the plane of the tetradentate dpp. Once again, it is possible for the resulting d^2 Ru^{VI} species to be either a low-spin singlet or an intermediate-spin triplet, and the calculations indicate that the triplet is more stable by ca. 6 kcal mol^{-1}. It should be noted that the species assigned as $(Ru^{VI}{=}O)^{4+}$ in this discussion has a resonance structure of $(Ru^{IV}O)^{4+}$. Finally, we explored the question of whether a stable $Ru^{IV}(OOH)^{3+}$ species could be formed by the reaction of a second water molecule with the $(Ru^{VI}{=}O)^{4+}$ complex and the elimination of a proton. The optimized structure of $[Ru^{IV}(OOH)(dpp)(pic)_2]^{3+}$ was calculated and is shown in Figure S5 in the Supporting Information. A similar calculation was carried out on complex **3a**, which appeared to be one of the least likely complexes to become seven-coordinate. After oxidation, that complex also became seven-coordinate. These preliminary calculations are consistent with the proposed mechanism for water oxidation and will be extended in future work to include solvation and characterization of the transition states.

Conclusions

Two closely related series of mononuclear ruthenium(II) polypyridine complexes have been prepared and thoroughly characterized by ^1H NMR, electronic absorption, and cyclic voltammetry. The absorption energies of the MLCT bands and the redox potentials of the complexes are consistent with their structures. Fourteen complexes are found to catalyze the decomposition of water resulting in the evolution of oxygen. TNs and rates are measured, but no clear correlation is found with substituent electronic effects [compare **3b** ($R = CH_3$ and **3d** ($R = NO_2$)]. On the other hand, chelate ring strain may play a role in that all of the active catalysts involved a tri- or tetradentate polypyridine ligand. However, this feature is not, in itself, a sole criterion for activity. The possible involvement of ruthenium dioxide was inconsistent with the kinetic profiles of some of the more active catalysts, and a catalyst recovery experiment did not indicate ligand loss or exchange. The reactions are unimolecular, and catalyst dimerization was ruled out by consideration of a di-*tert*-butyl-substituted derivative. A tentative mechanism involving a seven-coordinate ruthenium(IV) species is suggested where O−O bond formation occurs at a very electrophilic $Ru^{VI}{=}O$ bond. DFT calculations lend support to this proposed

mechanism.

Future studies will attempt to immobilize an effective catalyst on an electrode surface so that catalysis can be effected by the direct application of an electrochemical potential and the need for sacrificial cerium(IV) will be avoided. We are also considering the incorporation of an active catalyst into a molecular assembly that will ultimately lead to the *photochemical* decomposition of water and the evolution of both hydrogen and oxygen.

Experimental Section

The ^{1}H and ^{13}C NMR spectra were recorded on a General Electric QE-300 spectrometer at 300 and 75 MHz, respectively. Chemical shifts are referenced to the residual solvent peak and reported in parts per million. Electronic absorption spectra were recorded with a Varian Cary 50 Bio UV−visible spectrophotometer. All spectra were corrected for the background spectrum of the solvent. Mass spectra were obtained on a Thermo-Finnigan LCQ Deca XP Plus spectrometer. Cyclic voltammetric (CV) measurements were carried out with a BAS Epsilon electroanalytical system using a one-compartment cell equipped with a glassy carbon working electrode, a saturated calomel reference electrode (SCE), and a platinum wire as the auxiliary electrode. An acetonitrile solution of NBu_4PF_6 (0.1 M) in a tube with a porous glass frit on one end was used between the SCE electrode and the sample solution. CHN analyses were performed by Quantitative Technologies Inc., Whitehouse, NJ.

The rate of oxygen evolution was measured in a 10 mL round-bottomed flask with a threaded side arm for the introduction of an oxygen sensor probe. The flask was charged with $[Ce(NO_3)_6](NH_4)_2$ (550 mg, 1 mmol), and CF_3SO_3H(aq) (3 mL, adjusted to pH 1) was added to give a homogeneous solution, which was stirred at 20 °C in a temperature-controlled water bath. The complex (2.0×10^{-4} mmol) in a CH_3CN solution (50 μL) was injected into the cerium(IV) solution through a septum cap. The generated oxygen in the headspace of the flask was measured, and readings were recorded every 1 min for 20 h. The end-point oxygen content was also measured by GC to corroborate the oxygen sensor. The end-point oxygen generated was converted to TN and reported.

The oxygen sensor consists of an oxygen sensor probe (Ocean Optics FOXY-OR125-G) and a multifrequency phase fluorometer (Ocean Optics MFPF-100) interfaced to a PC. The raw data obtained by the fluorometer are monitored by the TauTheta Host Program. The data are then transferred to a percent O_2 reading by a program named "OOISensors". The GC is a Gow-Mac Series 400 thermal conductivity GC with an 8 ft. × $^1/_8$ in. 5 Å molecular sieve column operating at 70 °C and 20 mL min^{-1} of argon. The sample size is 100 μL, and air is used as the standard (21% O_2). The GC data are interfaced to a PC by a Gow-Mac program named "DACS".

Materials. 4-Picoline (pic; Aldrich), 2,2′-bipyridine (bpy; Aldrich), 4,4′-dimethyl-2,2′-bipyridine (dmbpy; Aldrich), 4,4′-dimethoxy-2,2′-bipyridine (dmxbpy; Acros), 1,10-phenanthroline (phen; TCI), 2,2′-biquinoline (biq; Lancaster), 2,2′-bipyrazine (bpz; Aldrich), 2,2′;6′,2″-terpyridine (tpy; GFS), $RuCl_3 \cdot xH_2O$ (Strem), and RuO_2 (Alfa Aesar) were purchased and used without further purification.

4,4′-Dinitro-2,2′-bipyridine (dnbpy),[21] diethyl-2,2′-bipyridine-4,4′-dicarboxylate (dedcbpy),[22] 1,1′-biisoquinoline (biiq),[23] 1,12-diazaperylene (dap),[24] 2,2′-bipyrimidine (bpm),[25] 2-(pyrid-2′-yl)-1,8-naphthyridine (pynap),[26] 4-aminopyrimidine-5-carbaldehyde,[27] 4-*tert*-butyl-2,6-diacetylpyridine,[28] $[Ru(DMSO)_4Cl_2]$,[29] $[Ru(bpy)(DMSO)_2Cl_2]$,[30] $[Ru(tpy)Cl_3]$,[31] $[Ru(tpy)(bpy)Cl](PF_6)$ (**3a**),[32] $[Ru(tpy)(dmbpy)Cl](PF_6)$ (**3b**),[33] $[Ru(tpy)(dmxbpy)Cl](PF_6)$ (**3c**),[34] $[Ru(tpy)(phen)Cl](PF_6)$ (**4**),[35] $[Ru(tpy)(biq)Cl](PF_6)$ (**5**),[36] $[Ru(tpy)(biiq)Cl](PF_6)$ (**6**),[37] $[Ru(tpy)(bpz)Cl](PF_6)$ (**8**),[38] $[Ru(tpy)(bpm)Cl](PF_6)$ (**9**),[39] *cis*-$[Ru(bpy)_2(pic)_2](PF_6)_2$ (**12**),[40] $[Ru(bpy)_3](PF_6)_2$ (**13**),[41] $[Ru(tpy)_2](PF_6)_2$ (**16**),[42] and $[Ru(dpp)(pic)_2](PF_6)_2$ (**17**)[43] (dpp = 2,9-dipyrid-2′-yl-1,10-phenanthroline) were synthesized according to published procedures. All other chemicals are commercially available, and all solvents are reagent grade.

$[Ru(tpy)(dnbpy)Cl](PF_6)$ (3d). $[Ru(tpy)Cl_3]$ (50 mg, 0.12 mmol) and dnbpy (29 mg, 0.12 mmol) were refluxed for 4 h in EtOH/H_2O (20 mL, 3:1) under argon. The reaction mixture was filtered hot, and the filtrate was evaporated to dryness. The solid was dissolved in a minimum amount of H_2O (3 mL), and an aqueous solution of NH_4PF_6 (50 mg in 2 mL) was added. The resulting precipitate was collected, washed with H_2O, and dried under vacuum overnight. The crude product was purified by chromatography on alumina, eluting with acetone/KPF_6 (200:1). The major band was collected and concentrated to provide a precipitate, which was collected, washed with H_2O, and dried under vacuum overnight. The solid was recrystallized from acetone/H_2O to provide a dark-brown powder (47 mg, 52%). ^{1}H NMR (CD_3CN): δ 10.58 (d, J = 6.0 Hz, 1H), 9.48 (d, J = 2.1 Hz, 1H), 9.18 (d, J = 2.1 Hz, 1H), 8.63 (dd, J = 6.0 and 2.1 Hz, 1H), 8.55 (d, J = 8.1 Hz, 2H), 8.41 (d, J = 8.4 Hz, 2H), 8.24 (t, J = 8.4 Hz, 1H), 7.94 (td, J = 8.1 and 1.2 Hz, 2H), 7.84 (d, J = 6.0 Hz, 1H), 7.65 (dd, J = 6.6 and 2.7 Hz, 1H), 7.56 (d, J = 5.4 Hz, 2H), 7.27 (ddd, J = 7.5, 5.4, and 0.9

(21) Maerker, G.; Case, F. H. *J. Am. Chem. Soc.* **1958**, *80*, 2745–2748.
(22) Mukkala, V. M.; Kankare, J. J. *Helv. Chim. Acta* **1992**, *75*, 1578–1592.
(23) Ashby, M. T.; Govindan, G. N.; Grafton, A. K. *J. Am. Chem. Soc.* **1994**, *116*, 4801–4809.
(24) Schmelz, O.; Mews, A.; Basché, T.; Herrmann, A.; Müllen, K. *Langmuir* **2001**, *17*, 2861–2865.
(25) Cai, C.; Lv, C. X. *Chin. J. Appl. Chem.* **2004**, *21*, 107–108.
(26) Campos-Fernández, C. S.; Thomson, L. M.; Galán-Mascarós, J. R.; Ouyang, X.; Dunbar, K. R. *Inorg. Chem.* **2002**, *41*, 1523–1533.
(27) Bell, T. W.; Beckles, D. L.; Debetta, M.; Glover, B. R.; Hou, Z.; Hung, K.-Y.; Khasanov, A. B. *Organic Preparations and Procedures International*, **2002**, *34*, 321−325.
(28) Nückel, S.; Burger, P. *Organometallics* **2001**, *20*, 4345–4359.
(29) Duliere, E.; Devillers, M.; Marchand-Brynaert, J. *Organometallics* **2003**, *22*, 804–811.
(30) Suzuki, T.; Kuchiyama, T.; Kishi, S.; Kaizaki, S.; Takagi, H. D.; Kato, M. *Inorg. Chem.* **2003**, *42*, 785–795.
(31) Sullivan, B. P.; Calvert, J. M.; Meyer, T. J. *Inorg. Chem.* **1980**, *19*, 1404–1407.
(32) Calvert, J. M.; Schmehl, R. H.; Sullivan, B. P.; Facci, J. S.; Meyer, T. J.; Murry, R. W. *Inorg. Chem.* **1983**, *22*, 2151–2162.
(33) Adcock, P. A.; Keene, F. R.; Smythe, R. S.; Snow, M. R. *Inorg. Chem.* **1984**, *23*, 2336–2343.
(34) Konno, H.; Kobayashi, A.; Sakamoto, K.; Fagalde, F.; Katz, N. E.; Saitoh, H.; Ishitani, O. *Inorg. Chim. Acta* **2000**, *299*, 155–163.
(35) Bonnet, S.; Collin, J. P.; Gruber, N.; Sauvage, J. P.; Schofield, E. R. *J. Chem. Soc., Dalton Trans.* **2003**, 4654–4662.
(36) Spek, A. L.; Gerli, A.; Reedijk, J. *Acta Crystallogr.* **1994**, *C50*, 394–397.
(37) Ashby, M. T.; Alguindigue, S. S.; Schwane, J. D.; Daniel, T. A. *Inorg. Chem.* **2001**, *40*, 6643–6650.
(38) Gerli, A.; Reedijk, J.; Lakin, M. T.; Spek, A. L. *Inorg. Chem.* **1995**, *34*, 1836–1843.
(39) Swavey, S.; Fang, Z.; Brewer, K. J. *Inorg. Chem.* **2002**, *41*, 2598–2607.
(40) Velders, A. H.; Massera, C.; Ugozzoli, F.; Biagini-Cingi, M.; Manotti-Lanfredi, A. M.; Haasnoot, J. G.; Reedijk, J. *Eur. J. Inorg. Chem.* **2002**, 193–198.
(41) Meyer, T. J.; Casper, J. V. *J. Am. Chem. Soc.* **1983**, *105*, 5583–5590.
(42) Norrby, T.; Borje, A.; Akermark, B.; Hammarström, L.; Alsins, J.; Lashgari, K.; Norrestam, R.; Martensson, J.; Stenhagen, G. *Inorg. Chem.* **1997**, *36*, 5850–5858.
(43) Zong, R.; Thummel, R. P. *J. Am. Chem. Soc.* **2004**, *126*, 10800–10801.

Hz, 2H). MS: *m/z* 616.3 $(M - PF_6)^+$. Anal. Calcd for $C_{25}H_{17}N_7O_4ClRuF_6P \cdot 0.5H_2O$: C, 39.01; H, 2.34; N, 12.74. Found: C, 38.93; H, 2.01; N, 12.30.

[Ru(tpy)(dedcbpy)Cl](PF$_6$) (3e). A mixture of [Ru(tpy)Cl_3] (110 mg, 0.25 mmol) and dedcbpy (75 mg, 0.25 mmol) in EtOH/H_2O (40 mL, 3:1) containing LiCl (10 mg) and Et_3N (0.2 mL) was refluxed overnight under argon. The reaction mixture was filtered hot. The filtrate was evaporated to dryness, the remaining solid was dissolved in a minimum amount of H_2O (5 mL), and an aqueous solution of NH_4PF_6 (100 mg in 3 mL) was added. The resulting precipitate was collected, washed with H_2O, and dried under vacuum overnight. The crude product was purified by chromatography on silica, eluting with acetone/KPF_6 (200:1). The major band was collected and concentrated to provide a solid, which was washed with H_2O and dried under vacuum overnight. The solid was recrystallized from acetone/H_2O to provide a dark-brown powder (122 mg, 60%). ^{1}H NMR (acetone-d_6): δ 10.54 (d, J = 5.7 Hz, 1H), 9.35 (d, J = 2.1 Hz, 1H), 9.07 (d, J = 2.1 Hz, 1H), 8.79 (d, J = 8.1 Hz, 2H), 8.65 (d, J = 7.5 Hz, 2H), 8.51 (dd, J = 5.7 and 1.5 Hz, 1H), 8.31 (t, J = 7.8 Hz, 1H), 8.03 (td, J = 7.5 and 1.5 Hz, 2H), 7.94 (d, J = 6.0 Hz, 1H), 7.84 (d, J = 5.4 Hz, 2H), 7.53 (dd, J = 6.3 and 1.8 Hz, 1H), 7.38 (ddd, J = 7.2, 5.7, and 1.2 Hz, 2H), 4.59 (q, J = 7.2 Hz, 2H), 4.34 (q, J = 7.2 Hz, 2H), 1.50 (t, J = 7.2 Hz, 3H), 1.29 (t, J = 7.2 Hz, 3H). Anal. Calcd for $C_{31}H_{27}N_5O_4ClRuF_6P$: C, 45.70; H, 3.32; N, 8.60. Found: C, 45.34; H, 3.24; N, 8.29.

[Ru(tpy)(dap)Cl](PF$_6$) (7). The procedure for [Ru(tpy)(dnbpy)-Cl](PF$_6$) was followed, using [Ru(tpy)Cl_3] (50 mg, 0.12 mmol) and dap (28 mg, 0.12 mmol). The crude product was purified by chromatography on alumina, eluting with acetone. The major green band was collected, and the solvent was evaporated. The solid was recrystallized from acetone/H_2O to provide **7** (61 mg, 72%). ^{1}H NMR (CD_3CN): δ 10.16 (d, J = 6.0 Hz, 1H), 8.77 (d, J = 7.5 Hz, 1H), 8.70 (dd, J = 5.7 and 2.4 Hz, 1H), 8.58 (d, J = 8.1 Hz, 2H), 8.40 (d, J = 6.3 Hz, 1H), 8.37 (d, J = 6.3 Hz, 2H), 8.33 (d, J = 8.4 Hz, 1H), 8.20 (t, J = 7.8 Hz, 1H), 8.07 (m, 2H), 7.84 (m, 3H), 7.50 (d, J = 5.4 Hz, 2H), 7.44 (d, J = 6.3 Hz, 1H), 7.36 (d, J = 7.2 Hz, 1H), 7.12 (ddd, J = 7.2, 5.4, and 0.6 Hz, 2H). MS: *m/z* 624.3 $(M - PF_6)^+$.

[Ru(tpy)(pynap)Cl](PF$_6$) (10). The procedure for [Ru(tpy)(d-edcbpy)Cl](PF$_6$) was followed, using [Ru(tpy)Cl_3] (100 mg, 0.23 mmol) and pynap (48 mg, 0.23 mmol). The crude product was purified by chromatography on alumina, eluting with acetone. The first band was collected, and the solvent was evaporated. The resulting solid was dissolved in CH_3CN (2 mL) and added to Et_2O (20 mL) dropwise. The resulting precipitate was collected and dried under vacuum overnight. The solid was recrystallized from acetone/H_2O to provide purple crystals (48 mg, 29%). ^{1}H NMR (acetone-d_6): δ 10.61 (dd, J = 5.7 and 1.5 Hz, 1H), 9.15 (d, J = 8.4 Hz, 1H), 8.79 (d, J = 8.1 Hz, 1H), 8.69 (d, J = 8.1 Hz, 2H), 8.50 (d, J = 8.1 Hz, 2H), 8.44 (td, J = 7.8 and 1.8 Hz, 1H), 8.41 (d, J = 8.1 Hz, 1H), 8.32 (dd, J = 8.7 and 1.8 Hz, 1H), 8.25 (dd, J = 4.5 and 1.8 Hz, 1H), 8.22 (t, J = 8.7 Hz, 1H), 8.11 (ddd, J = 7.2, 6.0, and 1.8 Hz, 1H), 7.87 (td, J = 8.1 and 2.1 Hz, 2H), 7.71 (dd, J = 5.4 and 1.5 Hz, 2H), 7.47 (dd, J = 7.2 and 4.8 Hz, 1H), 7.26 (ddd, J = 7.2, 5.4, and 1.2 Hz, 2H). MS: *m/z* 577.4 $(M - PF_6)^+$. Anal. Calcd for $C_{28}H_{20}N_6ClRuF_6P \cdot 0.5H_2O$: C, 46.03; H, 2.88; N, 11.51. Found: C, 46.16; H, 2.53; N, 11.26.

[Ru(bpy)(pic)$_4$](PF$_6$)$_2$ (11). A modified procedure for preparing [Ru(bpy)(py)$_4$](PF$_6$)$_2$ (py = pyridine) was followed.[44] A mixture of [Ru(bpy)(DMSO)$_2$Cl$_2$] (78 mg, 0.16 mmol) and pic (894 mg, 9.61 mmol) in H_2O (15 mL) was refluxed for 14 h under argon. The reaction mixture was filtered hot. The filtrate was allowed to cool to room temperature. An aqueous solution of NH_4PF_6 (163 mg in 3 mL) was added. The resulting precipitate was collected, washed with H_2O, and dried under vacuum overnight. The crude product was purified by chromatography on silica, eluting with acetone/hexanes (2:1). The major orange band was collected, and the solvent was evaporated. The resulting solid was recrystallized from acetone/H_2O to provide an orange-red powder (38 mg, 26%). ^{1}H NMR (acetone-d_6): δ 8.90 (d, J = 4.8 Hz, 2H), 8.69 (d, J = 7.8 Hz, 2H), 8.47 (d, J = 6.3 Hz, 4H), 8.19 (td, J = 7.5 and 0.9 Hz, 2H), 7.89 (d, J = 6.3 Hz, 4H), 7.74 (ddd, J = 7.2, 5.4, and 0.9 Hz, 2H), 7.48 (d, J = 6.0 Hz, 4H), 7.14 (d, J = 6.0 Hz, 4H), 2.50 (s, 6H), 2.31 (s, 6H). MS: *m/z* 775.3 $(M - PF_6)^+$, 315.3 $(M - 2PF_6)^{2+}$.

[Ru(tpy)(pic)$_3$](PF$_6$)$_2$ (14). A modified procedure for preparing [Ru(tpy)(4-ethylpyridine)$_3$](PF$_6$)$_2$ was followed.[45] A mixture of [Ru(tpy)Cl_3] (108 mg, 0.25 mmol), pic (1.5 g, 16.11 mmol), LiCl (20 mg), and Et_3N (0.3 mL) in EtOH/H_2O (30 mL, 5:1) was refluxed for 20 h under argon. The reaction mixture was filtered hot. The filtrate was evaporated to dryness, the remaining solid was dissolved in a minimum amount of H_2O (5 mL), and an aqueous solution of NH_4PF_6 (100 mg in 3 mL) was added. The resulting precipitate was collected, washed with H_2O, and dried under vacuum overnight. The crude product was purified by chromatography on silica, eluting with acetone and then acetone/H_2O (20:1). The major purple band was collected, and the solvent was evaporated. The solid was recrystallized from acetone/H_2O to provide a brown powder (211 mg, 95%). ^{1}H NMR (acetone-d_6): δ 8.98 (d, J = 4.2 Hz, 2H), 8.76 (d, J = 8.4 Hz, 2H), 8.74 (d, J = 8.7 Hz, 2H), 8.51 (d, J = 6.0 Hz, 2H), 8.29 (td, J = 8.1 and 1.8 Hz, 2H), 8.26 (t, J = 8.4 Hz, 1H), 7.90 (ddd, J = 7.8, 5.4, and 1.5 Hz, 2H), 7.66 (m, 6H), 6.99 (d, J = 6.6 Hz, 4H), 2.61 (s, 3H), 2.20 (s, 6H). Anal. Calcd for $C_{33}H_{32}N_6P_2F_{12}Ru$: C, 43.85; H, 3.54; N, 9.30. Found: C, 44.08; H, 2.79; N, 9.09.

[Ru(tpy)(bpy)(pic)](PF$_6$)$_2$ (15). A published procedure for preparing [Ru(tpy)(bpy)(py)](PF$_6$)$_2$ (py = pyridine) was followed.[46] A mixture of [Ru(tpy)(bpy)Cl](PF$_6$) (75 mg, 0.11 mmol) and pic (300 mg, 3.23 mmol) in EtOH/H_2O (30 mL, 1:1) was refluxed for 5 h under argon. The reaction mixture was filtered hot. The filtrate was evaporated to dryness, the remaining solid was dissolved in a minimum amount of H_2O (5 mL), and an aqueous solution of NH_4PF_6 (100 mg in 2 mL) was added. The resulting precipitate was collected, washed with H_2O, and dried under vacuum overnight. The crude product was purified by chromatography on silica, eluting with acetone/KPF_6 (50:1). The major band was collected and concentrated to provide a solid, which was washed with H_2O and dried under vacuum. The solid was recrystallized from acetone/H_2O to provide **15** (36 mg, 37%). ^{1}H NMR (acetone-d_6): δ 8.98 (d, J = 3.9 Hz, 1H), 8.95 (dd, J = 3.9 and 1.5 Hz, 1H), 8.85 (d, J = 7.8 Hz, 2H), 8.75 (d, J = 8.1 Hz, 2H), 8.70 (d, J = 7.5 Hz, 1H), 8.45 (td, J = 7.8 and 1.5 Hz, 1H), 8.37 (t, J = 7.8 Hz, 1H), 8.18 (td, J = 8.7 and 1.5 Hz, 2H), 8.11 (dd, J = 5.7 and 1.8 Hz, 2H), 8.00 (ddd, J = 8.1, 5.4, and 0.9 Hz, 1H), 7.95 (dd, J = 7.8 and 0.9 Hz, 1H), 7.84 (dd, J = 5.1 and 1.2 Hz, 2H), 7.63 (dd, J = 5.4 and 1.8 Hz, 1H), 7.58 (ddd, J = 8.1, 5.4, and 1.8 Hz, 2H), 7.23 (ddd,

(44) Wallin, S.; Davidsson, J.; Modin, J.; Hammarström, L. *J. Phys. Chem. A* **2005**, *109*, 4697–4704.

(45) Coe, B. J.; Thompson, D. W.; Culbertson, C. T.; Schoonover, J. R.; Meyer, T. J. *Inorg. Chem.* **1995**, *34*, 3385–3395.

(46) Hecker, C. R.; Fanwick, P. E.; McMillin, D. R. *Inorg. Chem.* **1991**, *30*, 659–666.

J = 7.2, 5.1, and 0.6 Hz, 1H), 7.19 (d, J = 6.3 Hz, 2H), 2.28 (s, 3H). Anal. Calcd for $C_{31}H_{26}N_6P_2F_{12}Ru$: C, 42.61; H, 2.98; N, 9.62. Found: C, 42.61; H, 2.44; N, 9.52.

2-Amino-6-*tert*-butylpyridine-3-carbaldehyde (21). To a solution of 4-aminopyrimidine-5-carbaldehyde (500 mg, 4.06 mmol) and pinacolone (450 mg, 4.50 mmol) in EtOH (20 mL) was added an EtOH solution of KOH (100 mg). The red solution was refluxed overnight. EtOH was evaporated, and the residue was purified by chromatography on silica gel, eluting with CH_2Cl_2 to give 7-*tert*-butylpyrido[2,3-*d*]pyrimidine (273 mg, 36%) as a yellow solid. ^{1}H NMR: δ 9.42 (s, 1 H), 9.35 (s, 1 H), 8.21 (d, J = 8.4 Hz, 1 H), 7.71 (d, J = 8.4 Hz, 1 H), 1.45 (s, 9 H). This material (273 mg, 1.46 mmol) in HCl (2M, 6 mL) was refluxed for 16 h, giving a red solution, which was neutralized with saturated aqueous $NaHCO_3$. The product was extracted with CH_2Cl_2 (3 × 10 mL). The organic extract was dried over Na_2SO_4 and evaporated to give an oil. Chromatography on alumina, eluting with CH_2Cl_2, afforded 2-amino-6-*tert*-butylpyridine-3-carbaldehyde as a white solid (150 mg, 21%). Mp 46−47 °C. ^{1}H NMR ($CDCl_3$): δ 9.76 (s, 1 H), 7.67 (d, J = 8.1 Hz, 1 H), 6.74 (d, J = 8.1 Hz, 1 H), 1.27 (s, 9 H). ^{13}C NMR ($CDCl_3$): δ 192.0, 175.7, 157.5, 144.1, 111.3, 108.6, 37.8, 29.6.

4-*tert*-Butyl-2,6-bis(7′-*tert*-butyl-1′,8′-naphthyrid-2′-yl)pyridine (23). A mixture of **21** (64 mg, 0.36 mmol), 4-*tert*-butyl-2,6-diacetylpyridine (**22**; 33 mg, 0.15 mmol), EtOH (10 mL), and KOH (50 mg) was refluxed overnight and then concentrated to about 1 mL. The solid material was collected, washed with EtOH and ether, and dried to afford **23** as a white solid (77 mg, 100%). Mp: 260−262 °C. ^{1}H NMR ($CDCl_3$): δ 8.93 (s, 2H), 8.91 (d, J = 8.7 Hz, 2H), 8.30 (d, J = 7.8 Hz, 2H), 8.16 (d, J = 8.7 Hz, 2H), 7.64 (d, J = 8.7 Hz, 2H), 1.55 (b, 27H). ^{13}C NMR ($CDCl_3$): δ 173.7, 162.3, 159.6, 155.0, 154.7, 137.2, 136.8, 120.8, 120.7, 120.0, 119.5, 38.7, 35.7, 30.8, 30.0. FTIR (ATR, cm^{-1}): 2966(w), 2227(w), 1608(s), 1599(s), 1538(m), 1504(s), 1117(s), 859(vs), 733(vs), 725(vs).

[Ru(23)(pic)$_2$(H$_2$O)](PF$_6$)$_2$ (24). A mixture of **23** (58.6 mg, 0.117 mmol) and $Ru(DMSO)_4Cl_2$ (58.6 mg, 0.119 mmol) in ethylene glycol (3 mL) was heated to reflux in a microwave oven for 10 min to produce a red solution. To the solution were added LiCl (10 mg), Et_3N (0.1 mL), 4-methylpyridine (0.3 mL, 3.0 mmol), H_2O (3 mL), and EtOH (5 mL). The mixture was refluxed for 26 h to afford a blue solution, which was extracted with CH_2Cl_2 (3 × 10 mL). The addition of NH_4PF_6 (105 mg, 0.64 mmol) to the aqueous solution produced a precipitate, which was collected, washed with H_2O, and dried. Chromatography on alumina, eluting with acetone, followed by a mixture of saturated aqueous KPF_6 and acetone (2:100), gave [Ru(**23**)(pic)$_2$(H$_2$O)](PF$_6$)$_2$ as a solid (71 mg, 55%). ^{1}H NMR (acetone-d_6): δ 9.89 (s, 1 H), 9.14 (d, J = 8.7 Hz, 2 H), 9.11 (s, 2 H), 8.90 (d, J = 9.6 Hz, 2 H), 8.77 (d, J = 8.1 Hz, 2 H), 8.22 (d, J = 8.4 Hz, 2 H), 7.91 (d, J = 6.6 Hz, 4 H), 6.81 (d, J = 6.0 Hz, 4 H), 2.07 (s, 6 H), 1.70 (s, 18 H), 1.62 (s, 9 H). The singlet at δ 9.89 disappeared when a drop of D_2O was added to the sample, indicating that the peak was due to coordinated H_2O. Anal. Calcd for $C_{45}H_{53}F_{12}N_7OP_2Ru\cdot 0.5KPF_6$: C, 45.38; H, 4.48; N, 8.23. Found: C, 45.55; H, 4.38; N, 7.84.

X-ray Crystallographic Determination of 10. All measurements were made with a Siemens SMART platform diffractometer equipped with a 4K CCD APEX II detector. A hemisphere of data (1271 frames at a 6 cm detector distance) was collected using a narrow-frame algorithm with scan widths of 0.30° in ω and an exposure time of 25 s frame^{-1}. The data were integrated using the Bruker-Nonius *SAINT* program, with the intensities corrected for the Lorentz factor, polarization, air absorption, and absorption due to variation in the path length through the detector faceplate. A Ψ-scan absorption correction was applied based on the entire data set. Redundant reflections were averaged. Final cell constants were refined using 8130 reflections having $I > 10\sigma(I)$, and these, along with other information pertinent to data collection and refinement, are listed in Table 4. The Laue symmetry was determined to be *mmm*, and from the systematic absences noted, the space group was shown unambiguously to be *Pbcn*. The PF_6 anion was found to be disordered over two slightly different orientations, having approximate occupancies of 70:30. These were refined as ideal rigid bodies. A molecule of solvent was located disordered about a 2-fold site and is presumed to be water. The isotropic displacement factor indicates that this molecule is only present half of the time (pop = 0.25); however, it is possible that some solvent was lost during handling, and so for all calculations the solvent site is presumed to be fully occupied (pop = 0.5).

Table 4. Crystallographic Data for Complex **10**·$^1/_2$H$_2$O

empirical formula	$C_{28}H_{21}ClF_6N_6O_{0.5}PRu$
fw	731.00
space group	*Pbcn* (orthorhombic)
unit cell constants	a = 29.8331(11) Å
	b = 8.7588(3) Å
	c = 21.1705(8) Å
	α = 90°
	β = 90°
	γ = 90°
formula units per cell	Z = 8
volume	5531.9(3) Å^3
density	ρ = 1.755 mg m^{-3}
abs coeff	μ = 0.796 mm^{-1}
R1	0.0296
wR2	0.0722

DFT Calculations. Electronic structure calculations were carried out at the DFT level of theory with the B3LYP functional,[47] as implemented in the *Gaussian 03* program package.[48] The LANL2DZ basis set was used for ruthenium and all other atoms.[49]

Acknowledgment. We thank the Robert A. Welch Foundation (E-621) and the Division of Chemical Sciences, Office of Basic Energy Sciences, U.S. Department of Energy (Contract DE-FG03-02ER15334 to H.-W.T., R.Z., and R.T. and Contract DE-AC02-98CH10886 to Brookhaven National Laboratory) for financial support of this work. We also thank Dr. James Korp for assistance with the X-ray determination and Dr. Zhongping Ou for help with the spectroelectrochemistry.

Supporting Information Available: X-ray crystallographic files for **10** (in CIF format), NMR spectra of **3a** and the recovered catalyst (Figure S1), spectroelectrochemical analysis of **3a** (Figure S2), and figures associated with DFT calculations (Figures S3−S5). This material is available free of charge via the Internet at http://pubs.acs.org.

IC8014817

(47) (a) Becke, A. D. *Phys. Rev. A* **1988**, *38*, 3098. (b) Lee, C.; Yang, W.; Parr, R. G. *Phys. Rev. B* **1988**, *37*, 785. (c) Miehlich, B.; Savin, A.; Stoll, H.; Preuss, H. *Chem. Phys. Lett.* **1989**, *157*, 200.

(48) Frisch, M. J.; et al. *Gaussian 03*, D.01 ed.; Gaussian, Inc.: Wallingford, CT, 2004.

(49) (a) Hay, P. J.; Wadt, W. R. *J. Chem. Phys.* **1985**, *82*, 270. (b) Hay, P. J.; Wadt, W. R. *J. Chem. Phys.* **1985**, *82*, 299. (c) Wadt, W. R.; Hay, P. J. *J. Chem. Phys.* **1985**, *82*, 284. (d) Dunning, T. H. J.; Hay, P. J. *Modern Theoretical Chemistry*; Plenum: New York, 1976.